Unmixing Progradational Sediments in a Southwestern Caribbean Gulf through Late Holocene: Backwash of Low-Level Atmospheric Jets

Authors: Rúa, Alex, Liebezeit, Gerd, Molina, Ruben, and Palacio, Jaime

Source: Journal of Coastal Research, 32(2) : 397-407

Published By: Coastal Education and Research Foundation

URL: https://doi.org/10.2112/JCOASTRES-D-14-00216.1

Journal of Coastal Research	32	2	397–407	Coconut Creek, Florida	March 2016

Unmixing Progradational Sediments in a Southwestern Caribbean Gulf through Late Holocene: Backwash of Low-Level Atmospheric Jets

Alex Rúa[†]*, Gerd Liebezeit[‡], Ruben Molina[§], and Jaime Palacio[†]

[†]GAIA, Corporación Académica Ambiental
Universidad de Antioquia UdeA
Medellín, Colombia

[‡]Institut für Chemie und Biologie des Meeres (ICBM)
Oldenburg Universität
Wilhelmshaven 268382, Germany

[§]GeoLimna, Escuela Ambiental
Facultad de Ingeniería
Universidad de Antioquia UdeA
Medellín, Colombia

www.cerf-jcr.org

www.JCRonline.org

ABSTRACT

Rúa, A.; Liebezeit, G.; Molina, R., and Palacio, J., 2016. Unmixing progradational sediments in a southwestern Caribbean gulf through late Holocene: Backwash of low-level atmospheric jets. *Journal of Coastal Research,* 32(2), 397–407. Coconut Creek (Florida), ISSN 0749-0208.

In the last few years there has been considerable interest in the assessment of the role of tropical seas in driving paleoclimate. Despite this interest, little is known about the evolution of progradational sediments near the Panama Isthmus during the late Holocene. This paper shows the dispersion assessment of fluvial sediments into a gulf from the southwestern Caribbean on a decadal-centennial scale as recorded in three sediment cores spanning between 300 and 960 ± 35 calibrated YBP. According to end-member modeling of size classes, sediments largely comprised clay, clayey fine silt, and silty mud that flocculated by differential settling. Coarsened facies were consistent with enhanced fluvial discharge owing to increased precipitation in the circum-Caribbean. Remarkably, decreased fluvial discharge into the gulf due to aridity in the Caribbean was modulated by oceanic moisture conveyed by the low-level atmospheric jets of Panama and CHOCO. Fluvial sediments may surely fail to contribute to shoreline stability because of muddy hinterland lithology.

ADDITIONAL INDEX WORDS: *Granulometry, end-member modeling, sedimentation rate, delta progradation, Little Ice Age, Medieval Warm Period.*

INTRODUCTION

Sediment transport is the response to complex interactions among atmospheric, oceanic, and terrestrial processes. In the southern Caribbean and across the eastern equatorial Pacific, the atmospheric low-level jets Panama and CHOCO control oceanic evaporation and precipitation patterns (Amador *et al.*, 2006; Martínez *et al.*, 2003). The low-level, jets-driven precipitation increases the flow energy of Andean rivers on a local scale (Poveda, Waylen, and Pulwarty, 2006). Many studies have demonstrated that increased energy enhances the capacity to entrain coarse-grained sediment into fluvial flow (Allison *et al.*, 2003; French, 1997; Kukal, 1990; Prandle, 2009; Prothero and Schwab, 2004). The result is that sedimentary features of drilled cores on seabed can be used as proxies for transport capacity of sediment from freshwater streams into coastal zones.

As energy of fluvial flow due to storms increases, progradational facies become coarser. A featured deltaic sequence of progradational facies comprises laminated layers of sand scattered through silty muds (Le Roux and Rojas, 2007; Prothero and Schwab, 2004). However, paleoceanographic reconstructions based merely on granulometry of muddy facies is considered difficult, even spurious (Schieber, 1989; Schieber, Southard, and Thaisen, 2007), because no textural key links transport agent and depositional setting to granulometry (Allison *et al.*, 2003; Tucker, 2009).

Many stratigraphic studies have revealed mechanisms of sediment deposition and coastal morphology changes that reflect interactions among climatic, oceanographic, geological, and biological factors. In recent years, various mathematical approaches have been proposed to interpret accurately those mechanisms by discriminating granulometry of polymodal sediments (Påse, 1997; Purkait and Majumdar, 2014; Xiao *et al.*, 2009). Some of the approaches include using hyperbolic tangent functions, lognormal distribution fitting, and bilinear unmixing. Paleodeposits can be efficiently reconstructed through bilinear unmixing as proportional contributions to granulometry of a fixed number of end-members (EMs), which can help identify both morphogenetic facies and their agents of deposition, *viz.*, paleocurrents, dust transport, terrigenous supply, and de-icing (Dietze *et al.*, 2012; Prins *et al.*, 2002, 2007; Weltje, 1997).

Incipient paleoenvironmental data in low latitudes have impinged on establishing the role of basinal atmospheric circulation as a player in climate variability on local, regional, and global scales. Studies at the Panama Isthmus in the Gulf of Urabá, where a narrow (130-km) strip of land separates the Atlantic and Pacific oceans, have been restricted either to surface circulation in the Recent epoch or anthropic effects on sediment yield and dispersion, as well as on benthic fauna (Álvarez and Bernal, 2007; Andrade and Barton, 2000; Andrade, Barton, and Mooers, 2003; Blanco, 2009; Correa, Alcántara-Carrió, and González, 2005; Gómez and Bernal,

DOI: 10.2112/JCOASTRES-D-14-00216.1 received 28 October 2014; accepted in revision 19 March 2015; corrected proofs received 23 June 2015; published pre-print online 3 August 2015.
*Corresponding author: afruaca@gmail.com

2013; Montoya, 2010; Restrepo and Kjerfve, 2004; Restrepo *et al.*, 2006; Vann, 1959). Moreover, there is little research on differentiating the effects of anthropic activities from natural variability on sedimentation through the late Holocene (Ospina, Palacio, and Vásquez, 2014; Rúa, Liebezeit, and Palacio, 2014). None of these studies have assessed the sediment structure throughout the stratigraphic profile to account for the interactions between environmental factors and external climate forcers within long timescales. The lack of information on the temporal progression of progradational facies limits the understanding of climate variability across the coastal zones at the isthmus.

In this study, we present three progradational records of precipitation variability derived from the Gulf of Urabá, at the Panama Isthmus, covering a period of 1000 years. Granulometry, chronology, facies structures, and fossil content are used along with EM modeling to identify provenance of polymodal sediment and establish possible agents of deposition. The following sections begin by describing study area and methodology. Then, results are presented and discussed in light of increased energy of fluvial flow due to both documented patterns of precipitation variability through the late Holocene and anthropic activities.

Study Area

The Gulf of Urabá is at the Panama Isthmus between 7°54′–8°40′ N and 76°56′–77°23′ W (Figure 1) in the southern Caribbean atop the triple junction of the Nazca, Caribbean, and South America plates (González, Nuñez, and Paris, 1988). In the Gulf of Urabá, shoreline retreat has been enhanced by the poor lithological strength of its cliffs and marine terraces within the geosynclinal frame, which comprises highly fractured and weathered claystones and mudstones (Correa and Vernette, 2004; Thomas *et al.*, 2007b). Around 50% of the Caribbean coastline of Colombia comprises fragile geomorphological units such as hills, high alluvial and calcareous terraces, coral reefs, and mangrove estuaries (Robertson, Martínez, and Jaramillo, 2003). Plate tectonics in the southern littoral zone of the Caribbean causes diapirism and hydroisostacy (Correa and Vernette, 2004). Eustasy enhances local sea level rise and erosion susceptibility, as the continental shelf of South America along the Caribbean subsides at 0.7 mm/y (Page, 1983).

The bathymetry in the gulf is concave, averaging 25 m depth. The last glaciations of the Quaternary carved underwater canyons of 10–13 m depth along the shelf, whose western coastline is linked to 5500 km^2 of alluvial flood plains drained by the Atrato River (Chevillot *et al.*, 1993; Robins, 1978; Thomas *et al.*, 2007b). The valley of the Atrato River extends 500 km southwest of the gulf between the Western Cordillera and Pacific coastal range around 5° N. Although many small streams with high sediment yield drain into the gulf, *ca.* 86% of the total sediment load is supplied by the Atrato River (Restrepo and Kjerfve, 2004). This river drains 35,700 km^2 of the Darién rainforest on the Pacific before emptying into the Caribbean (Robins, 1978). The Atrato lobate six-channel delta projects from the southwest, displaying eroded banks and accreted fronts (Molina, Molina, and Chevillot, 1992).

Total annual precipitation is *ca.* 2500 mm/y within the gulf itself, but the upper reaches of the Atrato receive rates as high as 11,000 mm/y (Restrepo *et al.*, 2002). With an annual mean temperature of 27°C during the last century, and ranging from 19°C to 40°C (Thomas *et al.*, 2007b), the shifts in latitude of the intertropical convergence zone (ITCZ) result in regional precipitation changes (Haug *et al.*, 2001; Lonin and Vásquez, 2005) following two contrasting patterns: *rainy* (April–November) and *dry* seasons (January–March). During the last decade, rainfall has been *ca.* 80 mm/mo in the dry season and *ca.* 862 mm/mo in the rainy season (Restrepo, López, and Restrepo, 2009).

More moisture is being transported from the Atlantic to the Pacific in the atmosphere (Barange *et al.*, 2011; Broecker, Sutherland, and Peng, 1999). Precipitation of Pacific moisture conveyed by south winds associated with the low-level CHOCO jet, however, provides the Atlantic Ocean a backwash (Figure 1a). This backwash is ultimately provided through the freshwater jet of the Atrato River into the Caribbean. Northeast trade winds bend the freshwater jet southward during the dry season, causing surface salinity in Colombia Bay to drop to 2 practical salinity units (PSU). When northeast trade winds (4.0–9.4 m/s) shift southeast, heavy rainfalls increase freshets that carry silt, rafts of streamside vegetation, and other debris into the valley of the Atrato River. The resulting freshwater jet then veers northward, allowing surface salinity in Colombia Bay to increase up to 30 PSU. In the alluvial flood plains drained by the Atrato River, 700–2600 y of fossil record have been eroded under these conditions (Berrío, Behling, and Hooghiemstra, 2000; Urrego *et al.*, 2006). Bottom water in the Gulf of Urabá is otherwise marine and likely to be a stretch of the Panama Countercurrent (Andrade and Barton, 2000; Chevillot *et al.*, 1993). The microtidal pattern is mixed semidiurnal; average wave height is 0.53 m with 5-s periods (Molina, Molina, and Chevillot, 1992).

METHODS

This section is organized as follows: The first subsection describes the materials and methodology used to carry out this research in the field and the laboratory. In the second subsection a statistical approach is presented. The data treatment for EM modeling is outlined in the third subsection. A discussion of the mathematical tools for the EM model falls outside the scope of this paper. For a detailed review on this topic, see Weltje (1997).

Coring and Laboratory Work

Three sediment cores between 2.0- and 2.7-m length were recovered using a gravity piston corer with polyvinyl chloride tubing of 6.3 cm internal diameter on-board R/V *ARC-Quindío* in December 2009 (Figure 1). Inevitably, there were sedimentary hiatuses of 10 cm atop the León mouth core and of 5 cm atop the prodelta core because of their slurry consistency. An erosive marine terrace was later sampled on the eastern coast in February 2011 (Table 1). All samples were stored at 4°C while awaiting analysis.

The three cores were visually described in detail and subsequently cut into 5-cm slices that totaled 135 samples.

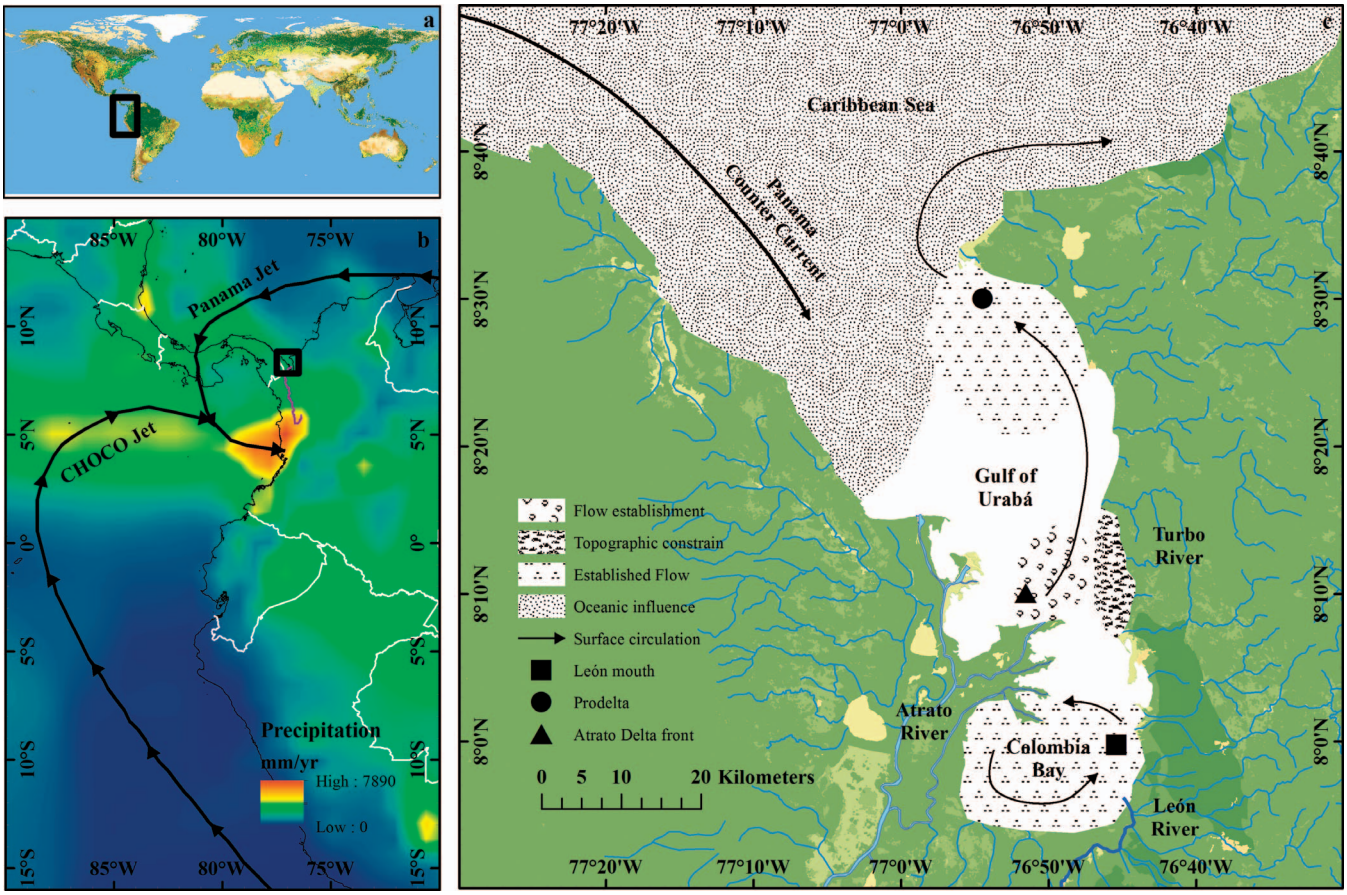

Figure 1. (a) World inset showing location of (b) Tropical South America (credit Wessel and Smith, 1996). Arrows represent wind streamlines associated with low-level CHOCO and Panama atmospheric jets (after Dee *et al.*, 2011). Meridional gradient of average multiannual precipitation at key sites is presented (Willmott and Webber, 1998). (c) Location of the Gulf of Urabá coastline at the Panama Isthmus showing the coring stations. Shaded areas represent hydrodynamic zonation, and arrows are surface circulation (adapted from Montoya, 2010).

After freeze drying at –40°C (Christ Alpha 1-4LSC), grain size distribution (0.15–540.21 μm) of samples was analyzed in triplicate with a Fritsch A22 laser particle size analyzer. Radiocarbon age of bulk sediment from León mouth and prodelta cores was analyzed at the Scottish Universities Environmental Research Centre based on accelerator mass spectrometry (Table 2). Age of the Atrato Delta front core is reconstructed from the mercury signal in sediments owing to gold amalgamation during the Spanish Conquest in Central America (Rúa, Liebezeit, and Palacio, 2014). Conventional ages were converted to calibrated ages using OxCal v3.1 (Ramsey, 2005) and mainly used for estimating sedimentation rates.

Table 1. *Coring locations and water depth at each sampling site.*

Sample Feature	Coordinates[a] N	Coordinates[a] W	Water Depth (m)	Sediment Section (m)
León Mouth	07°59′45″	76°45′24″	16	2.6
Prodelta	08°30′02″	76°54′28″	34	2.15
Atrato Delta Front	08°10′02″	76°51′33″	31	2.0
Erosive Terrace	8°13′6″	76°45′13″	—	—

[a] WGS84.

Statistics

For statistical analysis, the main variable of this study is averaged grain size (ϕ). To correlate size classes, grain size distribution was divided into five fractions: clay ($\phi < 2.0$ μm), fine silt ($2.0 < \phi < 6.3$ μm), medium silt ($6.3 < \phi < 20.0$ μm), coarse silt ($20.0 < \phi < 63.0$ μm), and sand ($63.0 < \phi < 500$ μm). Two-tailed Pearson or Spearman tests ($p < 0.01$) was used to correlate variables after testing for normality by Kolmogorov–Smirnov with the Lilliefors correction or Shapiro–Wilk test ($p < 0.05$). Finally, an analysis of variance was performed with the average grain size as a within-core factor.

End-Member Modeling Analysis of Grain Size Distributions

In an attempt to characterize the major components of sedimentary sources integrated in each coring site, robust EM analysis was performed by EMMAgeo (Dietze and Dietze, 2013). This model allowed us to decompose the three sets of compositional data by eigenspace analysis, data scaling, normalization, and factor rotation (Dietze *et al.*, 2012; Weltje, 1997). The input data for the model were cast in one matrix per coring site with m observations and n variables restricted to

Table 2. *Radiocarbon dates and $\delta^{13}C$ values of selected charcoal samples from cores recovered in the León mouth and prodelta in the Gulf of Urabá.*

Core	Depth (cm)	$\delta^{13}C$ (‰)	^{14}C Age (^{14}C YBP)	Calibrated YBP	Calendar Years
León Mouth	92	−32.3	125 ± 35	150	1800
	112	−30.4	135 ± 40	170	1780
	205	−25.0	230 ± 35	220	1730
Prodelta	49	−27.3	140 ± 35	160	1790
	113	−32.0	390 ± 35	430	1520
	200	−30.1	960 ± 35	870	1080

nonnegative values. The row elements $i = 1, 2, \ldots, m$ of each matrix were mean volume percentages of $j = 1, 2, \ldots, n$ grain size classes concerning the ith slice of the corresponding core. The j elements of each row i were added to 100%. Matrix dimension was 52×62 for the León mouth, 41×62 for the prodelta, and 40×49 for the Atrato Delta front. Because 13 columns of the latter matrix contained zeros alone, they were deleted to avoid model instabilities and redundancies. By running the model, we were consequently able to find a fixed number of EMs that held the major proportional contributions to the observed granulometry in each core.

RESULTS

This section is divided into the same three subsections as the methods. The key results of this study are: predicting major sources of sediment and unmixing the anthropic signal from long-term natural variability recorded in progradational facies.

Coring and Laboratory Work

The laminated clayey, very fine silt, fine silt, and sandy mud in the León mouth and prodelta cores were only correlated back to 300 ^{14}C YBP (Figure 2). They initially appear highly correlated. However, careful observation of chronology revealed that gross rate of sedimentation at the León mouth (1 cm/y) appeared to be up to five times as fast as on the prodelta during 960 ± 35 ^{14}C YBP. On the delta front, uncorrelated facies accreted rapidly from 0.18 cm/y in the bottom core up to 2.7 cm/y during the last *ca*. 70 calibrated (cal) YBP. Seven sedimentary facies were identified from the upper 2.7 m of the stratigraphic section in the three cores from the Gulf of Urabá based on sedimentary structures, median grain size, and fossil content. All cores were characterized by dark greenish-gray (56Y–4/1) laminations.

The terrigenous sediment coarsened toward the present, thereby substantiating northward progradation (Figures 2 and 3). Carbon isotope composition of bulk sediment ($\delta^{13}C < -25.0$‰) relative to the Vienna Pee Dee Belemnite confirmed its paramount terrigenous provenance (Table 2). Sand-laden events coincided with changes in facies (Figures 2 and 3). The sandy mud facies were reverse graded, with large sand grains projecting at the top and more mud at the bottom. In the bottom of the León mouth core, contributions of clay and fine silt increased in a long-term trend through the Little Ice Age (LIA), then plunged between 170 cal YBP (150 cm) and the present (top) owing to increased input of coarse silt and sand. Abundance of unidentified remains of bivalves, gastropods, echinoderms, and scaphopods increased downward in distal cores when rates of sedimentation were lowest, especially during the LIA. In contrast, facies thinned out laterally on the delta front and were devoid of fossils.

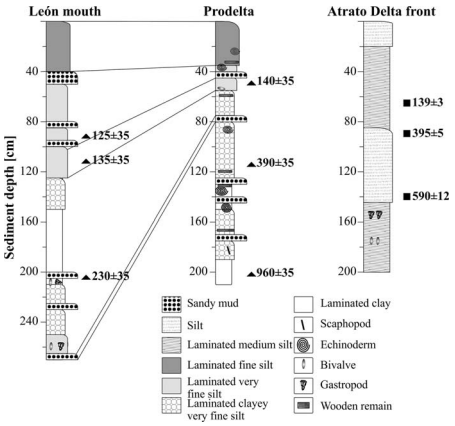

Figure 2. Lithology and chronology of the cores recovered in the Gulf of Urabá. ▲ Radiocarbon chronology. Deviation in estimates was expressed at the one sigma level of confidence, including components from the sample statistics, modern reference standard, and blank and random machine error. ■ Chronology based on history of Hg usage during colonial times (Rúa, Liebezeit, and Palacio, 2014).

Statistics

Our results suggest that the major tributary to the gulf (the Atrato River) supplied no sand. Despite this, the coarsest facies were found in the Atrato Delta front core, albeit with a paucity

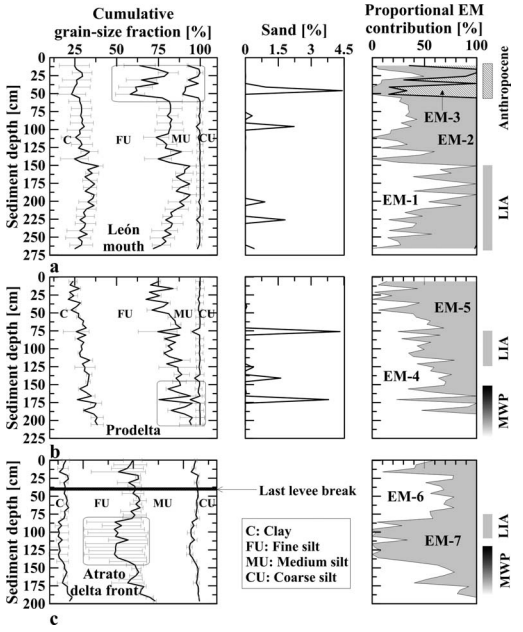

Figure 3. Individual grain size fractions and end-member reconstruction of recovered cores from the Gulf of Urabá in the (a) Leon mouth, (b) prodelta, and (c) Atrato Delta front. Error bars represent standard deviation of observations relative to results of end-member modeling. The Anthropocene, LIA, and MWP are shaded. Intense precipitation events depicted by sand peaks during the LIA coincide with other precipitation reconstructions in the circum-Caribbean region.

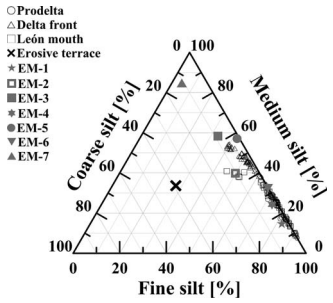

Figure 4. Shepard ternary diagram for silt contribution to end-members, erosive terrace, and seabed in the León mouth, prodelta, and Atrato Delta front from the Gulf of Urabá.

of sand (Figure 3). Here, high contributions both of medium and coarse silt prompted a significant reduction in fine silt ($p < 0.01$) between 70 and 150 cm. Input of medium silt explained up to 98.4% ($p < 0.01$) of granulometry changes in the prodelta core (Figure 3). Those changes correlated strongly with time ($0.82, p < 0.01$). As expected, marked peaks and lulls of medium silt caused changes in sedimentary facies. Further granulometry analysis of an erosive terrace showed that sediment load of tributaries was finer than deposits of marine terraces placed on the eastern backshore (Figure 4).

End-Member Modeling

The EMs were segregated into three lithological units regarding the distribution of their size classes: clay for EM-1 and EM-4; very fine silt for EM-2, EM-5, and EM-6; and muddy silt for EM-3 and EM-7 (Figures 5a–c). Interestingly, modal size of modeled EMs increased with distance to the deltaic front (Table 3). The modal size of EM-2 and EM-5 increased by 14% relative to EM-6, and modal size of EM-3 increased by 31% relative to EM-7. However, EM-3 appeared only in the anthropogenic strata atop the León mouth core (Figure 3). Only the León mouth core comprised three EMs that accounted for 91.6% of its granulometry changes (Figure 5d). The remaining two cores were effectively modeled by two EMs that accounted for at least 93.0% of their granulometry changes.

DISCUSSION

Results are interpreted in this section with regard to the basin reconstruction accomplished by EM modeling. Within the framework of these criteria, the first subsection discusses the implications for progradation of sedimentary facies. In the second subsection, an overview of hydrodynamics and implications for sediment transport and flocculation are given. The third subsection analyzes late Holocene sedimentation into the gulf, taking into account anthropic forcers. Finally, questions regarding the effect of low-level atmospheric jets on sedimentary facies are discussed in a broader context before drawing some conclusions.

Sedimentary Facies

The most remarkable result to emerge from EM modeling was predicting major sources of sediment that are dispersed into the basin. These major sources were silt and clay (Table 3).

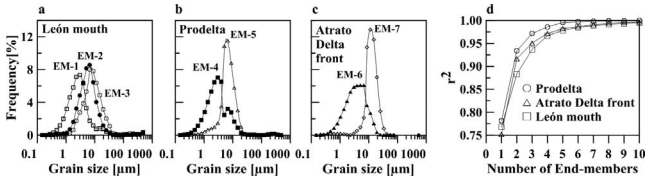

Figure 5. Unmixed distribution of end-member size classes for seabed sediments in the Gulf of Urabá: (a) León mouth, (b) prodelta, and (c) Atrato Delta front. (d) Performance of the end-member model.

This proved basinal dispersion of sediment. Wooden and echinoderm remains observed in the prodelta core clearly revealed that some clayey strata integrated marine and fluvial contributions (Figure 2), although fine-grained facies alone could conceal distinguishing features (Prothero and Schwab, 2004). Silt was the most conspicuous size class in the basin (Figure 3). From a modal class point of view, our results indicate that hinterland siltstone was composed of a very fine silt matrix enclosing a clayey-muddy framework (Table 3). This concurs well with hinterland forms (Vann, 1959) and also confirms that runoff transports eroded siltstone from the fissile hinterland in Urabá (Correa and Vernette, 2004). In fact, silt deposits in Urabá hinterland are derived mainly from basalt and andesite (Case *et al.*, 1971) transported to savannah fields from the valley of the Darién rainforest.

We found that grain size coarsened upward slightly with facies in a postglacial long-term trend through 960 ± 35 ^{14}C YBP. This reverse grading is interesting because of its significant correlation to chronology ($p < 0.05$). This correlation would imply that flow velocity during deposition within the Gulf of Urabá has slightly and steadily accelerated during the late Holocene as the delta prograded. Despite the increased flow velocity, fine silt contribution to sediment onto the gulf seabed was fairly constant through the late Holocene (Figure 3). Remarkably, the gulf remained a low-energy environment where sediment in all three cores was mainly fine silt. From local bathymetry and sedimentary facies, flow velocities driven on distal zones of the gulf (south and north) could be lower than on the delta front. This is shown by modeled hydrodynamics (Montoya and Toro, 2006) and prompt deposition both of coarse and medium silt on a decadal–centennial scale at the delta front (Figure 2). Furthermore, changes in medium and coarse silt ($r = -0.97, -0.55, p < 0.01$) mirrored changes in clay contribution (Figure 3). The last result is consistent with field studies indicating that clay enrichment on the continental slope, owing to the slightly accelerated flow, counteracts the

Table 3. *End-member modes and explained variance of three sediment cores recovered in the Gulf of Urabá.*

Coring Site	End-Member	Mode (μm)	Explained Variance (%)
León Mouth	1	2.64	76.3
	2	5.86	
	3	14.88	
Prodelta	4	2.64	80.0
	5	5.86	
Atrato Delta Front	6	5.13	72.3
	7	11.40	

import of more coarse and medium silt onto the gulf seabed (Pujos and Javelaud, 1991).

The temporal pattern of sand variation was discrete. Sandy mud facies in distal cores seemingly evinced strong input of bed load (Figure 2). Because strong storms may deposit sand layers atop finer sediment (Lick, 2010; Tucker, 2009; Xiao *et al.*, 2009), we believe the bed load input could also pertain to above-average flood stages of rivers caused by increased precipitation. Other studies in different deltas in the world have indicated that sand is supplied by their associated river (Allison *et al.*, 2003; Purkait and Majumdar, 2014; Restrepo and Kjerfve, 2004). However, if this were the case in the Gulf of Urabá, then the stratigraphic sequence of the delta front core also would have comprised sand (Figure 3). In fact, sediment in the lower reaches of the Atrato River is finer than in its upper reaches (Flórez *et al.*, 2005). This is because the feeble flow of this river (1.5 m/s) along a low gradient (3%) enhances coarse-grained deposition in Urabá backswamps, well before the gulf (Vann, 1959).

It thus appears that sand in the prodelta and León mouth cores was supplied by rivers other than the Atrato. Intermittent rivers provided a reliable explanation for this unusual result. They can carry virtually all its bed load at flood stage (Arroyave, Blanco, and Taborda, 2012) from sandy backshores on the east down to the seabed. After floods, laminated sands are deposited rapidly onto the prodelta by a single hydrodynamic event (Prothero and Schwab, 2004) and thereafter are buried by finer sediment during quiescent conditions (Lick, 2010).

Hydrodynamics

Hydrosedimentary fluxes of the Atrato, León, Turbo, and intermittent rivers converged with one another along the eastern shoreface (Figure 1). Flow pattern of river flumes within the gulf is hypopycnal. Modeled flow pattern of the Gulf of Urabá (Montoya and Toro, 2006) has shown that precipitation and wind direction force pronounced seasonal cycles in the salinity intrusion length. As a result, the locations of main depocenters alternate spatially (Vann, 1959) between the delta front and the Colombia Bay, owing to the seasonal meandering of the Atrato River freshwater jet. Meanwhile, seawater that mixes at the boundary of the freshwater jet is replaced by a shoreward flow in bottom water (Montoya, 2010), carrying the clayey EM-1 or EM-4. Yet the outflow of the freshwater jet is always ultimately pointed northeast regardless of the season, owing to topographic constraints, Coriolis force, and cyclonic vortexes (Álvarez and Bernal, 2007; Chevillot *et al.*, 1993; Montoya and Toro, 2006). This explains why the northwestern portion of the gulf has been little affected by terrigenous sedimentation, allowing coral reef development (Díaz, Díaz-Pulido, and Sánchez, 2000) through the Holocene. The hydrosedimentary fluxes were thus clearly integrated on the prodelta through the late Holocene.

Suspended sediment settles basically by gravity in zones of established flow when residual velocity is low (Bates, 1953; Montoya and Toro, 2006). To further illustrate local flow regimes and flocculation at each coring site, the Gulf of Urabá can be divided conveniently into five zones (Figure 1b): (1) zone of flow establishment on the Atrato Delta front, where Froude number (Fr) = 3.5, indicating supercritical flow; (2) zone of topographic constrain on eastern shore, where flow decelerated from 1.5 to 0.5 m/s and Fr = 0.7; (3, 4) two zones of established flow on the Colombia Bay and prodelta, where subcritical flow (Fr = 0.5) would be prominently influenced by wind drag and tidal currents; and (5) zone of oceanic influence to the northwest, where the Panama Countercurrent enters the gulf (Andrade, Barton, and Mooers, 2003). In zones of established flow, settling speed of flocs (W_s) is such that the Reynolds number is <0.5 (Lick, 2010). Consequently, Stokes law would explain our results for the León mouth and prodelta. It may be premature to reach such conclusions, and clearly there may be other possible interpretations for our findings. Further work should be devoted in improving the hydrodynamic model of the gulf to, for example, evaluate the necessary reduction in freshwater discharge into the gulf for allowing colonization of the Colombia Bay by both larvae of bivalves and gastropods during the LIA.

As fluvial sediment is spread over the surface of the basin seawater, it is widely distributed by basin water currents before reaching the seabed (Figure 1b; Case *et al.*, 1971; Prandle, 2009). In fact, sediment erosion and deposition are more directly linked to near-bed velocities than to the magnitude and direction of (depth-integrated) flows (Prandle, 2009). The lower reaches of the tributaries lack actual assessment both of sediment load and gauging of flow. Yet taking into account the proposed denudation of 315–700 t/km^2 per year (Restrepo and Kjerfve, 2000; Restrepo *et al.*, 2006), we estimated using the Judson and Ritter (1964) equation for erosion rates that local erosion across the Darién rainforest was slow (1.78–3.96 cm/ky) compared with (9.32 cm/ky) the erosion rate of Latin America (Kukal, 1990). Small Andean Rivers do denudate slowly (Pujos and Javelaud, 1991; Restrepo and Kjerfve, 2000), but their contribution to the global suspended load to the oceans remains elusive (Restrepo and Kjerfve, 2000). When land use (López and Blanco, 2008), local topography, and mineralogy are accounted for (Heitmuller and Hudson, 2009), the sediment yield in Urabá could sporadically be 10 times as high as we suggested (Blanco, 2009).

Although mud aggregates in clay balls and larger lumps are hardly surprising (Lick, 2010; Prothero and Schwab, 2004), the silty EM-6 flocculated prominently by differential settling in zones of established flow (Figure 6). The modal class of EM-6 on the Atrato Delta front was slightly finer than those of EM-2 on the León mouth and EM-5 on the prodelta (Table 3). Seen in this way, the EM model seems also to have reproduced sediment aggregation during transport. Ives (1978) proposes three mechanisms for particle collision that result in flocculation: Brownian motion (β_b), fluid shear (β_f), and differential settling (β_d). Fluid shear is usually dominant in many estuaries with high gradient velocities (Kranenburg, 1988; Shiono and West, 1987; West, Knight, and Shiono, 1984). By contrast, "current" gradient velocity ($G = 0.08$/s) estimated by Montoya and Toro (2006) in the Gulf of Urabá is comparatively low. Yet, given the steady increase in flow velocity inferred from the increased amount of silt through the late Holocene, this gradient velocity in the Recent epoch plausibly could have been the highest through the last 1000 y.

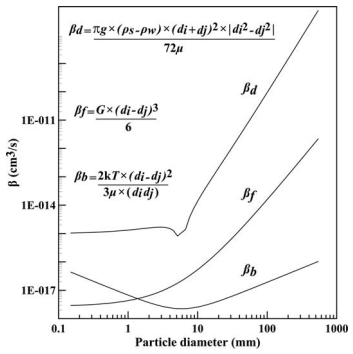

Figure 6. Collision function β as a function of particle size: collisions with a 5.13 μm particle (mode of EM-6). β_d, β_f, and β_b are the collision functions for differential settling, fluid shear, and Brownian motion, respectively. For these calculations, k is the Boltzmann constant (1.38×10^{-23} Nm/K), T is the absolute temperature of surface seawater in the gulf (303 K), μ is the dynamic viscosity of the surface seawater, d_i and d_j are the diameters of the colliding particles, G is the mean velocity gradient in the fluid (0.08/s), ρ_s and ρ_w are the densities of sediment and water, respectively ($\rho_s - \rho_w = 1.64$ g/cm^3), and g is the acceleration of gravity. All figures are from Montoya (2010), Montoya and Toro (2006), and Ospina (2012).

Unexpectedly, among our results, it was found that for the same sediment diameter, settling speed of flocs increases with sediment concentration and fluid shear (Burban *et al*., 1990). For EM-2 and EM-5 to comply with increased floc sizes, suspended sediment concentration must have ranged 24–37 mg/L in the León mouth and 15–22 mg/L in the prodelta through the late Holocene, as proposed by Lick, Huang, and Jepsen (1993) when assuming steady state for flocculating mud entering the sea. These concentrations were estimated from two physically based expressions. First, settling speed of flocs W_s is a function of median floc diameter d_s ($W_s = 0.145 d_s^{1.58}$). Second, median floc diameter is a function of the product between sediment concentration, C, and local fluid shear G ($d_s = 10.5[CG]^{-0.4}$). According to Schlichting (1955), the local fluid shear due to settling and associated drag on flocs is theoretically on the order of W_s/d_s. Settling speeds of flocs were thus calculated assuming the modal size class of EM-6 as the initial value for d_s.

Late Holocene Sedimentation and Anthropic Forcers

The paleodelta at the gulf entrance (55–60 m depth) was rapidly submersed at the time of sea level rise between 11,000 and 10,000 YBP (Pujos and Javelaud, 1991). Sedimentation rates in the gulf then varied widely within space and time. They have accelerated from 0.2 cm/y in the early Holocene to 1–8 cm/y in the late Holocene (Thomas *et al*., 2007a). One limitation of our age model was sample size. Clearly, three dated samples per core are not enough to picture a detailed climate reconstruction, so the long-term sedimentation rates in our age model should be considered rough averages. However, from the results of those nine dated samples and assuming steady state, a pattern of triggered sedimentation toward the present also emerged (Figure 2). Gross rate of sedimentation in the León mouth reached *ca*. 1 cm/y. This high rate is in agreement with bathymetric follow-up (Chevillot *et al*., 1993; Thomas *et al*., 2007a) and the cyclonic circulation on Colombia Bay (Molina, Molina, and Chevillot, 1992) causing a local turbidity maximum around the León mouth (Bernal *et al*., 2005). Other sedimentation triggers in the gulf have been (a) tsunamis like the one recorded in AD 1883 (Ménanteau, 2007), (b) extreme seismic activity (Restrepo *et al*., 2002), (c) subdelta exchanges with levee breaks in AD 1898 (Vann, 1959), and (d) expansion of banana cropland from 5000 to 33,790 ha throughout the 20th century (Blanco, 2009; Ménanteau, 2007). There is strong evidence for how sedimentation is affected by these climatic, geophysical, hydrographical, and hydrological factors (Pekar *et al*., 2004). In fact, vertical accretion on the delta front corresponded to 2.7 cm/y after the last levee break (Rúa, Liebezeit, and Palacio, 2014) and increased to 10–15 cm/y during the 20th century (Chevillot *et al*., 1993). In contrast, we found that average deposition rate in the prodelta was fairly constant (0.2 cm/y) through the late Holocene. Similarly, the mean sedimentation rate of the Amazon River was 0.5–1.15 cm/y during the Pleistocene and also dropped to 0.3 cm/y during the Holocene (Nitrouer *et al*., 1986).

Álvarez and Bernal (2007), Bernal *et al*. (2005), and Gómez and Bernal (2013) have reduced the sedimentary hiatus atop the León mouth core. They report that topset strata in Colombia Bay are devoid of benthic foraminifera owing to coarsened facies from medium silt to sand. This was the result of increased hydraulic energy due to anthropogenic factors. Most likely, the recent increased transport of eroded sandy mud depicted by EM-3 pertains to the expanded banana plantations on the León River basin (Figure 3a). Eroded soil in the gulf was deposited near the erosion site and not transported toward deeper water (Figure 4). Thus, another way to interpret the results from Álvarez and Bernal (2007) on sediment transport pathways into the gulf is that sand cascades down the sides of basin floor canyons, probably as a debris flow after strong storms.

In the Darién rainforest, *Zea mays* subsp. *mays* occurrence in palynological records corroborates human activity during at least the last 1000 calendar years (Berrío, Behling, and Hooghiemstra, 2000). Furthermore, anthropic activities induce continued change against a background of long-term environmental change entailing positive feedbacks for erosion (French, 1997), amplifying the climate response. The eastern coastline of the Gulf of Urabá retreated at rates of 1.3–2.5 m/y during the past four decades, because the municipality of Turbo was constructed on a mangrove swamp that formerly protected the coast from waves (Correa and Vernette, 2004). Those rates accelerated up to 40 m/y owing to the development of coastal defenses (Correa, Alcántara-Carrió, and González, 2005) by laypersons as a desperate measure to keep land from the sea.

Backwash Effect of Low-Level Jets on Fluvial Flow and Sedimentary Facies

Sand content in prodelta and León mouth cores may reflect intense rainfall events on the Urabá basin through the late Holocene. These events displayed 20–80 y of recurrence in the León mouth core compared with 100–200 y of recurrence in the relatively larger scale prodelta core (Figure 2). These differences could be attributed to dissimilarities in core resolution. In

fact, sand-laden strata between 950 and 650 cal YBP, around 430 cal YBP, and after 140 cal YBP relate to extremely wet periods in the Colombian Andes and the circum-Caribbean region (Broecker, 2001; Gischler *et al*., 2008; Lane *et al*., 2011; Urrego *et al*., 2006; van der Hammen and Cleef, 1992). Restrepo and Kjerfve (2004) and Arroyave, Blanco, and Taborda (2012) offer further indisputable evidence that fluvial discharge and sediment yield from Andean rivers of Colombia into the Caribbean change consistently with rainfall seasonality.

Interestingly, aridity throughout the LIA was punctuated by two extreme events of increased precipitation, as shown by two peaks of sand fraction in León mouth core (Figure 3). Similarly, Haug *et al*. (2001) found two peaks in Ti content in sediments that clearly show these two extreme precipitation events onto the Cariaco basin during the LIA. In this regard, our granulometric measurements showed two important results. First, our climate reconstruction concurred to some extent with other findings from the Caribbean. The long-term trend of clay enrichment displayed by EM-1 in the bottom León mouth core matches with higher evaporation–precipitation ratios in a large part of northern South America and the Caribbean up to 140 ^{14}C YBP through the LIA (Hodell *et al*., 2005; Mann *et al*., 2009; van der Hammen and Cleef, 1992). Second, the amplitude variation in size classes in the prodelta core was larger through the Medieval Warm Period (MWP) than the LIA. Remarkably, this finding did not fully agree with observations in the circum-Caribbean region (Gischler *et al*., 2008; Haug *et al*., 2001; Peterson and Haug, 2006). In fact, it is in good agreement with triggered precipitation on the Equatorial Pacific through the late Holocene (Conroy *et al*., 2008). This similarity suggests that precipitation forcing, found through our measurements, has been linked between the Pacific and the isthmus through the atmospheric low-level Panama and CHOCO jets.

Returning to the question posed at the beginning of this study, it is now possible to affirm that the "backwash" precipitation onto the Darién rainforest was sustained by evaporation in the Pacific and Atlantic oceans (Figure 1). Two low-level atmospheric jets carry this oceanic moisture from the Pacific (CHOCO jet) and the Atlantic (Panama jet). These two promote convergence of oceanic moisture over a 1500-m topographic low in the western Cordillera at 5° N on Colombian hinterland, thereby favoring massive precipitation (13,000 mm/y) on the upper reaches of the Atrato River (Poveda, Jaramillo, and Vallejo, 2014). Additionally, Poveda and Mesa (2000) have provided undeniable evidence that precipitation associated with jet convergence is stronger (weaker) when the ITCZ is south (north) of the Gulf of Urabá and the northeast trades intensify (weaken). Aridity across the Caribbean owing to southward migration of the ITCZ was thus essentially modulated by the condensation of oceanic moisture conveyed by the low-level jets through fluvial discharge into the Gulf of Urabá during the late Holocene. In line with previous studies (Amador *et al*., 2006; Koutavas *et al*., 2002; Martínez *et al*., 2003), the facies alternation in our progradational record was thus prominently influenced by precipitation and meridional circulation, which in turn are affected by the El Niño Southern Oscillation (ENSO).

When the ITCZ migrates between about 10° N over the Caribbean and equatorial Pacific, both meridional precipitation and runoff increase on this spot (Figure 1). As discussed, Haug *et al*. (2001) results in marine sediment from the Cariaco basin of Venezuela align with reconstructed precipitation in the circum-Caribbean region. At the same time, these results show a reverse correlation with reconstructed precipitation on the eastern Pacific (Betancourt *et al*., 2000; Conroy *et al*., 2008). Consequently, our results reflect the proposal in which precipitation onto and runoff from northern South America into the Caribbean decreased during the late Holocene, owing to more southerly positions of the ITCZ and increased ENSO frequency (Haug *et al*., 2001; Peterson and Haug, 2006; Sachs *et al*., 2009).

CONCLUSIONS

Linkages between the low-level atmospheric Panama and CHOCO jets with ENSO must be accounted for when it comes to progradation in the Gulf of Urabá, owing to its geographic position. If we defined silt (EM-2, EM-5, and EM-7) coarsening of the seabed as an environmental response to increased precipitation during the late Holocene, river runoff was a positive feedback. This highlighted the atmospheric backwash for low-level Panama and CHOCO jets in playing both roles negative through the LIA and positive through the MWP. As estimated, low rates of erosion (1.78–3.96 cm/ky) were triggered by massive precipitation (1837–12,717 mm/y) and expanded banana cropland around the Darién rainforest, which resulted in steadily increased fluvial energy parallel to enhanced export of riverborne mud to the Caribbean. Our results, however, favor the conclusion that freshwater discharge of the Atrato River into the gulf could not have applied fluid shear on the León mouth and prodelta through the late Holocene. Unfortunately, the mud surplus failed to contribute to littoral stability, but to siltation in the Colombia Bay and delta front, while clay was progressively not allowed to settle onto the prodelta.

According to the reconstruction of three sediment cores, the Gulf of Urabá seabed comprised mainly fluvially contributed clay, very fine clayey silt, and sandy mud mixed with marine clay, seemingly supplied by the Panama Countercurrent. A progradating pattern emerged from the alternation of upward coarsened laminated facies, reminiscent of slow steady deposition. Despite this, shoreline moved landward through the Anthropocene owing to subsidence of the Caribbean shelf (Page, 1983) coupled with shore abrasion (Correa, Alcántara-Carrió, and González, 2005). Furthermore, marine facies transgressed rapidly across the gulf throughout the LIA, as depicted by gastropod fossils (Ospina, Palacio, and Vásquez, 2014) and increased contribution of fine-grained sediments EM-1, EM-4, and EM-6. We have demonstrated that sand supply did not rely on the Atrato River flume, owing to the silty hinterland and backswamp deposition, but on shore abrasion and extreme precipitation events. Although some progress has been made when unmixing sediment, this incremental approach could not discern accurately terrigenous from marine clay. However, future work based on this study will look into carbon isotopes (^{13}C) in gulf sediments. Further work should be devoted to establishing the extent of the atmospheric backwash

from the Pacific as delivered by the CHOCO jet into the southern Caribbean.

ACKNOWLEDGMENTS

This research was made possible by a grant from the Colombian Administrative Department of Science, Technology and Innovation (COLCIENCIAS) and was partly sponsored by the Centre of Excellence in Marine Sciences (CEMarin). We thank the Universities Antioquia, Eafit, and Nacional de Colombia for donating the sediment cores to the CEMarin. We warmly thank Dr. I. Correa, L.C. Giraldo, J.B. Ospina, and C.A. Vélez for helping out with data collection. Thanks are also due to Dr. M.T. Flórez, who gave us much valuable advice in early stages of this work.

LITERATURE CITED

Allison, M.A.; Khan, S.R.; Goodbred, S.L., Jr., and Kuehl, S.A., 2003. Stratigraphic evolution of the late Holocene Ganges–Brahmaputra lower delta plain. *Sedimentary Geology,* 155(3), 317–342.

Álvarez, A.M. and Bernal, G.R., 2007. Estimación del campo de transporte neto de sedimentos en el fondo de Bahía Colombia con base en análisis de tendencia del tamaño de grano. *Avances en Recursos Hidráulicos,* 16(October), 41–50.

Amador, J.A.; Alfaro, E.J.; Lizano, O.G., and Magaña, V.O., 2006. Atmospheric forcing of the eastern tropical Pacific: A review. *Progress in Oceanography,* 69(2–4), 101–142.

Andrade, C.A. and Barton, E.D., 2000. Eddy develompment and motion in the Caribbean Sea. *Journal of Geophysical Research,* 105(C11), 26191–26201.

Andrade, C.A.; Barton, E.D., and Mooers, C.N.K., 2003. Evidence for an eastward flow along the Central and South American Caribbean Coast. *Journal of Geophysical Research,* 108(C6), 1–11.

Arroyave, A.; Blanco, J.F., and Taborda, A., 2012. Exportación de sedimentos desde cuencas hidrográficas de la vertiente oriental del Golfo de Urabá: Influencias climáticas y antrópicas. *Revista de Ingenierías: Universidad de Medellín,* 11(20), 13–30.

Barange, M.; Field, J.G.; Harris, R.P.; Hofmann, E.E.; Perry, R.I., and Werner, F.E., 2011. *Marine Ecosystems and Global Change*. Wiltshire, U.K.: Oxford University Press, 440p.

Bates, C.C., 1953. Rational theory of delta formation. *Bulletin of the American Association of Petroleum Geologists,* 37(9), 2119–2162.

Bernal, G.R.; Montoya, L.J.; Garizábal, C., and Toro, M., 2005. La complejidad de la dimensión física en la problemática costera del Golfo de Urabá, Colombia. *Gestión y Ambiente,* 8(1), 123–135.

Berrío, J.C.; Behling, H., and Hooghiemstra, H., 2000. Tropical rainforest history from the Colombian Pacific area: A 4200-year pollen record from Laguna Jotaordó. *The Holocene,* 10(6), 749–756.

Betancourt, J.L.; Latorre, C.; Rech, J.A.; Quade, J., and Rylander, K.A., 2000. A 22,000-year record of monsoonal precipitation from northern Chile's Atacama Desert. *Science,* 289(5484), 1542–1546.

Blanco, J.F., 2009. Banana crop expansion and increased river-borne sediment exports to the Gulf of Urabá, Caribbean coast of Colombia. *Ambio,* 38(3), 181–183.

Broecker, W.S., 2001. Was the medieval warm period global? *Science,* 291(5508), 1497–1499.

Broecker, W.S.; Sutherland, S., and Peng, T.H., 1999. A possible 20th-century slowdown of Southern Ocean deep water formation. *Science*, 286(5442), 1132–1135.

Burban, P.Y.; Xu, Y.J.; McNeil, J., and Lick, W., 1990. Settling speeds of flocs in fresh water and seawater. *Journal of Geophysical Research: Oceans (1978–2012),* 95(C10), 18213–18220.

Case, J.E.; Durán, L.G.; López, S.; Alfonso, R., and Moore, W.R., 1971. Tectonic investigations in western Colombia and eastern Panama. *Geological Society of America Bulletin,* 82(10), 2685–2712.

Chevillot, O.; Molina, A.; Giraldo, L., and Molina, C., 1993. Estudio geológico e hidrológico del Golfo de Urabá. *Boletín Científico CIOH,* 14(July), 79–89.

Conroy, J.; Overpeck, J.T.; Cole, J.E.; Shanahan, T.M., and Steinitz-Kannan, M., 2008. Holocene changes in eastern tropical Pacific climate inferred from a Galápagos lake sediment record. *Quaternary Science Reviews,* 27(11–12), 1166–1180.

Correa, I.D.; Alcántara-Carrió, J., and González, R.D.A., 2005. Historical and recent shore erosion along the Colombian Caribbean Coast. *In:* Alcántara-Carrió, J. and Tena, J. (eds.), *Coastal Erosion: Proceedings of the II Meeting in Marine Sciences, 6th–8th May 2004, Valencia, Spain*. Journal of Coastal Research, Special Issue No. 49, pp. 52–57.

Correa, I.D. and Vernette, G., 2004. Introducción al problema de la erosión litoral en Urabá (sector Arboletes-Turbo) costa caribe colombiana. *Boletín de Investigaciones Marinas y Costeras,* 33(1), 7–28.

Dee, D.P.; Uppala, S.M.; Simmons, A.J.; Berrisford, P.; Poli, P.; Kobayashi, S.; Andrae, U.; Balmaseda, M.A.; Balsamo, G.; Bauer, P.; Bechtold, P.; Beljaars, A.C.M.; van de Berg, L.; Bidlot, J.; Bormann, N.; Delsol, C.; Dragani, R.; Fuentes, M.; Geer, A.J.; Haimberger, L.; Healy, S.B.; Hersbach, H.; Hólm, E.V.; Isaksen, L.; Kållberg, P.; Köhler, M.; Matricardi, M.; McNally, A.P.; Monge-Sanz, B.M.; Morcrette, J.-J.; Park, B.-K.; Peubey, C.; de Rosnay, P.; Tavolato, C.; Thépaut, J.N., and Vitart, F., 2011. The ERA-Interim reanalysis: Configuration and performance of the data assimilation system. *Quarterly Journal of the Royal Meteorological Society,* 137(656), 553–597.

Díaz, J.M.; Díaz-Pulido, G., and Sánchez, J.A., 2000. Distribution and structure of the southernmost Caribbean coral reefs: Golfo de Urabá, Colombia. *Scientia Marina,* 64(3), 327–336.

Dietze, E.; Hartmann, K.; Diekmann, B.; IJmker, J.; Lehmkuhl, F.; Opitz, S.; Stauch, G.; Wünnemann, B., and Borchers, A., 2012. An end-member algorithm for deciphering modern detrital processes from lake sediments of Lake Donggi Cona, NE Tibetan Plateau, China. *Sedimentary Geology,* 243–244, 169–180.

Dietze, M. and Dietze, E., 2013. *EMMAgeo: End-Member Modelling Algorithm and Supporting Functions for Grain-Size Analysis*. http://www.inside-r.org/packages/emmageo/versions/0-9-1.

Flórez, M.T.; González, J.; Arias, L.A.; Roy, K.; Palacio, J.; Aguirre, N.J.; Zárate, C.A., and Zuiliani, S., 2005. *Cartografía del Medio Natural y sus Alteraciones Antrópicas en el Parque Nacional Natural Los Katíos, Departamentos de Antioquia y Chocó, Colombia*. Medellín, Colombia: Universidad de Antioquia, Ministerio de Educación-UNESCO, 174p.

French, P.W., 1997. *Coastal and Estuarine Management*. London: Routledge Environmental Management Series, 251p.

Gischler, E.; Shinn, E.A.; Oschmann, W.; Fiebig, J., and Buster, N.A., 2008. A 1500-year Holocene Caribbean climate archive from the Blue Hole, Lighthouse reef, Belize. *Journal of Coastal Research,* 24(6), 1495–1505.

Gómez, E. and Bernal, G.R., 2013. Influence of the environmental characteristics of mangrove forests on recent benthic foraminifera in the Gulf of Urabá, Colombian Caribbean. *Ciencias Marinas,* 39(1), 69–82.

González, H.; Nuñez, A., and Paris, G., 1988. *Mapa geológico de Colombia, memoria explicativa*. Bogotá, Colombia: Ingeominas, scale 1:1,500,000, 8–11.

Haug, G.H.; Hughen, K.A.; Sigman, D.M.; Peterson, L.C., and Röhl, U., 2001. Southward migration of the intertropical convergence zone through the Holocene. *Science,* 293(5533), 1304–1308.

Heitmuller, F.T. and Hudson, P.F., 2009. Downstream trends in sediment size and composition of channel-bed, bar, and bank deposits related to hydrologic and lithologic controls in the Llano River watershed, central Texas, USA. *Geomorphology,* 112(3), 246–260.

Hodell, D.A.; Brenner, M.; Curtis, J.H.; Medina-Gonzalez, R.; Can, E.I.C.; Albornaz-Pat, A., and Guilderson, T.P., 2005. Climate change on the Yucatan Peninsula during the Little Ice Age. *Quaternary Research,* 63(2), 109–121.

Ives, K.J., 1978. *The Scientific Basis of Flocculation*. Alphen aan den Rijn, The Netherlands: Springer, 372p.

Judson, S. and Ritter, D.F., 1964. Rates of regional denudation in the United States. *Journal of Geophysical Research,* 69(216), 3395–3401.

Koutavas, A.; Lynch-Stieglitz, J.; Marchitto, T.M., Jr., and Sachs, J.P., 2002. El niño–like pattern in ice age tropical Pacific sea surface temperature. *Science,* 297(5579), 226–230.

Kranenburg, C., 1988. Long internal waves and turbulence production in estuarine flows. *Estuarine, Coastal and Shelf Science,* 27(1), 15–32.

Kukal, Z., 1990. How are rates of geological processes measured and expressed? *Earth-Science Reviews,* 28(1–3), 10–258.

Lane, C.S.; Horn, S.P.; Orvis, K.H., and Thomason, J.M., 2011. Oxygen isotope evidence of Little Ice Age aridity on the Caribbean slope of the Cordillera Central, Dominican Republic. *Quaternary Research,* 75(3), 461–470.

Le Roux, J.P. and Rojas, E.M., 2007. Sediment transport patterns determined from grain size parameters: Overview and state of the art. *Sedimentary Geology,* 202(3), 473–488.

Lick, W., 2010. *Sediment and Contaminant Transport in Surface Waters*. Boca Raton, Florida: CRC Press, 389p.

Lick, W.; Huang, H., and Jepsen, R., 1993. Flocculation of fine-grained sediments due to differential settling. *Journal of Geophysical Research: Oceans (1978–2012),* 98(C6), 10279–10288.

Lonin, S. and Vásquez, J.G., 2005. Hidrodinámica y distribución de coliformes en el Golfo de Urabá. *Boletín Científico CIOH,* 23, 76–89.

López, S.R. and Blanco, J.F., 2008. Illicit crops in tropical America: Deforestation, landslides and the terrestrial carbon stocks. *Ambio,* 37(2), 141–143.

Mann, M.E.; Zhang, Z.; Rutherford, S.; Bradley, R.S.; Hughes, M.K.; Shindell, D.; Ammann, C.; Faluvegi, G., and Ni, F., 2009. Global signatures and dynamical origins of the Little Ice Age and Medieval Climate Anomaly. *Science,* 326(5957), 1256–1260.

Martínez, I.; Keigwin, L.; Barrows, T.T.; Yokohama, Y., and Southon, J., 2003. La niña–like conditions in the eastern equatorial Pacific and a stronger Choco jet in the northern Andes during the last glaciation. *Paleoceanography,* 18(2), 11-1–11-18.

Ménanteau, L., 2007. Geohistoria del golfo. *In:* García-Valencia, C. (ed.), *Atlas del golfo de Urabá: Una mirada al Caribe de Antioquia y Chocó*. Santa Marta, Colombia: Serie de Publicaciones Especiales de Invemar No. 12, pp. 23–74.

Molina, A.; Molina, C., and Chevillot, P., 1992. La percepción remota aplicada para determinar la circulación de las aguas superficiales del Golfo de Urabá y las variaciones de su línea de costa. *Boletín Científico CIOH,* 11(July), 43–58.

Montoya, L.J., 2010. Dinámica Oceanográfica del Golfo de Urabá y su Relación con los Patrones de Dispersión de Contaminantes y Sedimentos. Medellín, Colombia: Universidad Nacional de Colombia, Ph.D. dissertation, 254p.

Montoya, L.J. and Toro, F.M., 2006. Calibración de un modelo hidrodinámico para el estudio de los patrones de circulación en el Golfo de Urabá, Colombia. *Avances en Recursos Hidráulicos,* 13, 37–54.

Nitrouer, C.A.; Kuehl, S.A.; Demaster, D.J., and Kowsmann, R.C., 1986. The deltaic nature of Amazon shelf sedimentation. *Geological Society of America Bulletin,* 97(4), 444–458.

Ospina, J., 2012. Los Moluscos como Bioindicadores de las Condiciones Ambientales durante el Holoceno Tardío en el Golfo de Urabá, Colombia. Medellín, Colombia: Universidad de Antioquia, Master's thesis, 178p.

Ospina, J.; Palacio, J., and Vásquez, L.F., 2014. ¿Responden los micromoluscos a los cambios ambientales durante el Holoceno tardío en el sur del mar Caribe colombiano? *Universitas Scientiarum,* 19(3), 233–246.

Page, W.D., 1983. Holocene deformation of the Caribbean coast, northwestern Colombia. Field trip C: General geology, geomorphology and neotectonics of northwestern Colombia. (Appendix) *Transactions of the 10th Caribbean Geological Conference* (Cartagena, Colombia), pp. 1–20.

Påse, T., 1997. Grain size distributions expressed as *tanh*-functions. *Sedimentology,* 44(6), 1011–1014.

Pekar, S.F.; McHugh, C.M.G.; Christie-Blick, N.; Jones, M.; Carbotte, S.M.; Bell, R.E., and Lynch-Stieglitz, J., 2004. Estuarine processes and their stratigraphic record: Paleosalinity and sedimentation changes in the Hudson Estuary (North America). *Marine Geology,* 209(1–4), 113–129.

Peterson, L.C. and Haug, G.H., 2006. Variability in the mean latitude of the Atlantic Intertropical Convergence Zone as recorded by riverine input of sediments to the Cariaco basin (Venezuela). *Palaeogeography, Palaeoclimatology, Palaeoecology,* 234(1), 97–113.

Poveda, G.; Jaramillo, L., and Vallejo, L.F., 2014. Seasonal precipitation patterns along pathways of South American low-level jets and aerial rivers. *Water Resources Research,* 50(1), 98–118.

Poveda, G. and Mesa, O.J., 2000. On the existence of Lloró (the rainiest locality on Earth): Enhanced ocean-land-atmosphere interaction by a low-level jet. *Geophysical Research Letters,* 27(11), 1675–1678.

Poveda, G.; Waylen, P.R., and Pulwarty, R.S., 2006. Annual and interannual variability of the present climate in northern South America and southern Mesoamerica. *Palaeogeography, Palaeoclimatology, Palaeoecology,* 234(1), 3–27.

Prandle, D., 2009. *Estuaries: Dynamics, Mixing, Sedimentation and Morphology*. Cambridge, U.K.: Cambridge University Press, 248p.

Prins, M.A.; Bouwer, L.M.; Beets, C.J.; Troelstra, S.R.; Weltje, G.J.; Kruk, R.W.; Kujipers, A., and Vroon, P.Z., 2002. Ocean circulation and iceberg discharge in the glacial North Atlantic: Inferences from unmixing of sediment size distributions. *Geology,* 30(6), 555–558.

Prins, M.A.; Vriend, M.; Nugteren, G.; Vandenberghe, J.; Lu, H.; Zheng, H., and Weltje, G.J., 2007. Late Quaternary aeolian dust input variability on the Chinese Loess Plateau: Inferences from unmixing of loess grain-size records. *Quaternary Science Reviews,* 26(1), 230–242.

Prothero, D.R. and Schwab, F., 2004. *Sedimentary Geology: An Introduction to Sedimentary Rocks and Stratigraphy*. New York: Macmillan, 557p.

Pujos, M. and Javelaud, O., 1991. Depositional facies of a mud shelf between the Sinú River and the Darién Gulf (Caribbean coast of Colombia): Environmental factors that control its sedimentation and origin of deposits. *Continental Shelf Research,* 11(7), 601–623.

Purkait, B. and Majumdar, D.D., 2014. Distinguishing different sedimentary facies in a deltaic system. *Sedimentary Geology,* 308(1), 53–62.

Ramsey, C.B., 2005. *OxCal v3.1.* https://c14.arch.ox.ac.uk/embed.php?File=oxcal.html.

Restrepo, J.D. and Kjerfve, B., 2000. Water discharge and sediment load from the western slopes of the Colombian Andes with focus on Río San Juan. *The Journal of Geology,* 108(1), 17–33.

Restrepo, J.D. and Kjerfve, B., 2004. The Pacific and Caribbean rivers of Colombia: Water discharge, sediment transport and dissolved loads. *In:* de Lacerda, L.D.; Santelli, R.E.; Duursma, E.K., and Abrao, J.J. (eds.), *Environmental Geochemistry in Tropical and Subtropical Environments*. Berlin: Springer, pp. 169–187.

Restrepo, J.D.; Kjerfve, B.; Correa, I.D., and González, J., 2002. Morphodynamics of a high discharge tropical delta, San Juan River, Pacific coast of Colombia. *Marine Geology,* 192(4), 355–381.

Restrepo, J.D.; López, S.A., and Restrepo, J.C., 2009. The effects of geomorphic controls on sediment yield in the Andean Rivers of Colombia. *Latin American Journal of Sedimentology and Basin Analysis,* 16(2), 79–92.

Restrepo, J.D.; Zapata, P.; Díaz, J.M.; Garzón-Ferreira, J., and García, C.B., 2006. Fluvial fluxes into the Caribbean Sea and their impact on coastal ecosystems: The Magdalena River, Colombia. *Global and Planetary Change,* 50(1–2), 33–49.

Robertson, K.; Martínez, N.J., and Jaramillo, O., 2003. Amenazas naturales asociadas al ascenso del nivel del mar en el Caribe colombiano. *Cuadernos de Geografía,* 12(1–2), 135–153.

Robins, C.R., 1978. Fisheries potential of the Gulf of Urabá. *Proceedings of the Thirtieth Annual Gulf and Caribbean Fisheries Institute and the Conference on Development of Small-Scale Fisheries in the Caribbean Region* (Miami, Florida, Gulf and Caribbean Fisheries Institute), pp. 71–74.

Rúa, A.; Liebezeit, G., and Palacio, J., 2014. Mercury colonial footprint in Darién Gulf sediments, Colombia. *Environmental Earth Sciences,* 71(4), 1781–1789.

Sachs, J.P.; Sachse, D.; Smittenberg, R.H.; Zhang, Z.; Battisti, D.S., and Golubic, S., 2009. Southward movement of the Pacific intertropical convergence zone AD 1400–1850. *Nature Geoscience,* 2(7), 519–525.

Schieber, J., 1989. Facies and origin of shales from the mid-Proterozoic Newland Formation, Belt Basin, Montana, USA. *Sedimentology,* 36(2), 203–219.
Schieber, J.; Southard, J., and Thaisen, K., 2007. Accretion of mudstone beds from migrating floccule ripples. *Science,* 318(5857), 1760–1763.
Schlichting, H., 1955. *Boundary-Layer Theory*. New York: McGraw-Hill, 817p.
Shiono, K. and West, J.R., 1987. Turbulent perturbations of velocity in the Conwy estuary. *Estuarine, Coastal and Shelf Science,* 25(5), 533–553.
Thomas, Y.F.; Cesaraccio, M.; García-Valencia, C., and Ménanteau, L., 2007a. Contribution of historical hydrography to the sea bottom cinematic study: Evolution of the Urabá Gulf Colombia. *Boletín Científico CIOH,* 25(December), 110–119.
Thomas, Y.F.; García-Valencia, C.; Cesaraccio, M., and Rojas, X., 2007b. El paisaje en el Golfo. *In:* García-Valencia, C. (ed.), *Atlas del golfo de Urabá: Una mirada al Caribe de Antioquia y Chocó*. Santa Marta, Colombia: Serie de Publicaciones Especiales de Invemar No. 12, pp. 75–128.
Tucker, M.E., 2009. *Sedimentary Petrology: An Introduction to the Origin of Sedimentary Rocks*. Trenton, New Jersey: Wiley, 272p.
Urrego, L.E.; Molina, L.A.; Urrego, D.H., and Ramírez, L.F., 2006. Holocene space–time succession of the Middle Atrato wetlands, Chocó biogeographic region, Colombia. *Palaeogeography, Palaeoclimatology, Palaeoecology,* 234(1), 45–61.
van der Hammen, T. and Cleef, A.M., 1992. Holocene changes of rainfall and river discharge in northern South America and the El Niño phenomenon. *Erdkunde Band,* 46(3/4), 252–256.
Vann, J.H., 1959. Landform–vegetation relationships in the Atrato delta. *Annals of the Association of American Geographers,* 49, 345–360.
Weltje, G.J., 1997. End-member modeling of compositional data: Numerical-statistical algorithms for solving the explicit mixing problem. *Mathematical Geology,* 29(4), 503–549.
Wessel, P.A. and Smith, W.H.F., 1996. Global self-consistent, hierarchical, high-resolution shoreline database. *Journal of Geophysical Research,* 101(B4), 8741–8743.
West, J.R.; Knight, D.W., and Shiono, K., 1984. A note on flow structure in the Great Ouse estuary. *Estuarine, Coastal and Shelf Science,* 19(3), 271–290.
Willmott, C.J. and Webber, S.R., 1998. *South American Precipitation: Gridded Monthly and Annual Climatologies (Version 1.02)*. http://climate.geog.udel.edu/~climate/html_pages/README.sa.p.cl.html.
Xiao, J.; Chang, Z.; Wen, R.; Zhai, D.; Itoh, S., and Lomtatidze, Z., 2009. Holocene weak monsoon intervals indicated by low lake levels at Hulun Lake in the monsoonal margin region of northeastern Inner Mongolia, China. *The Holocene,* 19(6), 899–908.